Hindawi
International Journal of Chemical Engineering
Volume 2022, Article ID 1929350, 8 pages
https://doi.org/10.1155/2022/1929350

Research Article

Applying Optimized ANN Models to Estimate Dew Point Pressure of Gas Condensates

Luo Han[1] and Saeed Sarvazizi[2,3]

[1]*School of Computer, Jiangsu University of Science and Technology, Zhenjiang, Jiangsu Province 212003, China*
[2]*Department of Petroleum Engineering, Ahwaz Faculty of Petroleum Engineering, Petroleum University of Technology (PUT), Ahwaz, Iran*
[3]*Department of Petroleum Engineering, Amirkabir University of Technology (Tehran Polytechnic), Tehran, Iran*

Correspondence should be addressed to Saeed Sarvazizi; sarvazizi.saeed@aut.ac.ir

Received 1 February 2022; Revised 9 February 2022; Accepted 20 March 2022; Published 1 April 2022

Academic Editor: Andreas Bück

It is economically and technically essential to promptly and accurately estimate the dew point pressure (DPP) of gas condensate to, for example, characterize fluids, evaluate the performance of reservoirs, plan and develop reservoirs for gas condensates, and design/optimize a production system. Indeed, it is difficult to experimentally explore the DPP. Furthermore, experimental tests are time-consuming and complicated. Therefore, it is required to develop an accurate, reliable DPP estimation framework. This paper introduces artificial neural network (ANN) models coupled with optimization algorithms, including a genetic algorithm (GA) and particle swarm optimization (PSO), for DPP estimation. A total of 721 data points were employed to train and test the algorithm. In addition, the outlier data were identified and excluded. The root-mean-squared error (RMSE) and the coefficient of determination (R^2) were calculated to be 230.42 and 0.982 for the PSO-ANN model and 0.0022 and 0.997 for the GA-ANN model, respectively. The model estimates were found to be in good agreement with the experimental dataset. Therefore, it can be said that the proposed method is efficient and effective.

1. Introduction

A gas-liquid ratio from 3.2 to 150 MCF/STB is applied to the reservoirs of gas condensates [1, 2]. A drip in the pressure in the vicinity of the wellbore below the dew point pressure (DPP) would diminish the efficiency of the reservoir [3–5]. Moreover, the transferability of gases near the well and permeability effectiveness decline when the condensates are partially blocked [6, 7]. Hence, the separation of the gases within the reservoir in the vicinity of the wellbore leads to smaller fractions of the produced gas [8, 9]. It is crucial to accurately and promptly estimate PPD in order to, for example, characterize fluids, evaluate the performance of a reservoir, design and develop reservoirs for gas condensates, and design and develop a production system [10, 11]. Despite significant accuracy and reliability, it is costly and time-consuming to experimentally measure the DPP [12].

As experimental processes may be sometimes infeasible, accurate and simple estimation models are to be developed. The equation of state (EoS) approach is an effective methodology. However, to implement EoS models, it is required to accurately characterize the fraction of heptane plus (C_{7+}) [13, 14].

Researchers introduced numerous DPP estimation models of gas condensates, e.g., EoS, graphical, and artificial intelligence (AI) models. Eilerts and Smith explored the relationships of the DPP with the composition, temperature, oil-gas volume ratio, and molal average boiling point (MABP) [15]. Olds et al. investigated reservoir fluids of the Paloma field and reported that the composition had a significant effect on the DPP [16].

Reamer and Sage sought to develop a model for the purpose of extending the formulations to larger gas-oil ratios using a total of five sample pairs of a field in Louisiana [17].

They emphasized that parameters other than the gas-oil ratio were involved in the composition effects. Organick and Golding introduced a straightforward model for saturation pressure estimation of volatile oil mixtures and gas condensates [18]. They reported that the composition and saturation pressure were directly associated. The modified weight average equivalent molecular weight and MABP were utilized as generalized characteristics of the composition independent of hydrocarbon equilibrium constants. Nemeth and Kennedy estimated the DPP based on the composition, C_{7+}, and temperature [19]. Crogh enhanced the formulation of Nemeth et al. by relating the depleting composition of a mixture of retrograde gas condensates to the composition at the DPP [20].

Potsch and Braeuer graphically estimated the DPP at a maximum error of 5 bars (<3%) [21]. Carlson and Cawston found that the DPP was dependent on the H_2S concentration [22]. Elsharkway used gas temperature and compositions of routine measurement to empirically estimate the DPP of gas condensates and demonstrated that the model outperformed EoS approaches [23]. Marruffo et al. introduced a DPP estimation correlation based on eighty PVT data points [24]. The maximum error was found to be 5.74%. The inputs included the gas condensate ratio, C_{7+} concentration, temperature, and API gravity. The model was implemented on fifty-four data points and was demonstrated to outperform the model of Nemeth [25]. González et al. proposed a DPP prediction neural network for reservoirs of retrograde gases using a total of 802 constant volume depletion data points [26]. The mean absolute error was calculated to be 8.74%.

In recent years, the use of new methods of modeling and data analysis to facilitate the solution of complex problems has attracted the attention of many researchers [27–32] and the use of artificial intelligence and machine learning methods have found many applications [33–38]. Artificial intelligence methods have been introduced in various sciences and disciplines and have been able to answer many previously unresolved problems [39–42]. Jalili et al. proposed a number of artificial neural network (AAN) models for DPP estimation using a total of 111 data points [43]. The highest training performance was observed for the Levenberg-Marquardt algorithm. Al-Dhamen and Al-Marhoun used nonlinear multiple regression, ANN, and alternating conditional expectation (ACE) algorithms based on a constant mass expansion test dataset of fields in the Middle East [1]. They found that the ANN model outperformed the nonlinear multiple regression and ACE algorithms. Godwin developed a model for the DPP estimation of gas condensates based on 259 data points [44]. The model was reported to outperform the existing approaches. Alzahabi et al. exploited a dataset of downhole fluid analysis to develop a new correlation [45].

The present work aims to comprehensively review and evaluate the gas condensate DPP literature. Two new models of PSO-ANN and GA-ANN are introduced to this aim and compared to earlier studies. 721 datasets were collected from other sources [46]. The collected data are subjected to data cleansing. We used 75% of them for the training stages and the rest for the testing stages. Then, models were created. Finally, various statistical analyzes have been used to evaluate the proposed models.

2. ANN

An ANN learns from experience for the purpose of performance improvement and adaptation [47, 48]. An ANN model consists of connected operating components (neurons) in a number of layers. Radial basis functions (RBFs) and multilayer perceptrons (MLPs) are the most common ANN classes [49]. An MLP includes an input layer, one or more hidden layers, and an output layer. The layers contain a number of neurons. It is required to implement the optimal number of hidden layer neurons [50]. MLP handles equivalent problem variables, and the interconnections are employed to train the model. It should be mentioned that an efficient MLP architecture requires optimized interconnections [51].

A hybrid RBF-ANN algorithm would be simpler than an MLP-ANN framework [52]. These models can effectively respond to patterns outside the training dataset. An RBF-ANN design is dependent on iteratively estimating localized basis function networks [53]. The RBF-ANN approach is more rapid and straightforward and, therefore, is preferable over the MLP-ANN methodology [54]. The RBF-ANN architecture consists of input, hidden, and output layers. The hidden layer nodes are subjected to RBFs. The nonlinear activation function serves as a neuron. The parameters include the RBF center, distance scale, and precise shape. The parameters undergo adjustment once it is linear. The RBF-ANN approach could produce an optimal solution to adaptable weights at the minimum MSE. Let x be the input pattern. The RBF-ANN output is given by [55]

$$y_i(x) = \sum_{k=1}^{h} w_{ki} \varnothing\left(\left\|x - x_k\right\|\right), \tag{1}$$

where x_k denotes the center archetype of hidden unit k, w_{ki} represents the weight of the connection between hidden unit k and output i, and symbol $\|\cdot\|$ represents the Euclidean norm. In addition, RBF (φ) is the Gaussian function. For scalar input, the Gaussian is included in equation (2) (as a representative radial function) [56].

$$h(x) = \exp\left(\frac{-(x-c)^2}{r^2}\right). \tag{2}$$

The Gaussian RBF parameters include the radius r and the center c. The Gaussian RBF reduces monotonically as the distance from the center rises. In contrast, a multiquadric RBF monotonically increases as the distance from the center increases (for scalar inputs) [57].

$$h(x) = \frac{\sqrt{r^2 + (x-c)^2}}{r}. \tag{3}$$

In contrast to the universal response of multiquadric RBFs, a Gaussian RBF is local with further common uses.

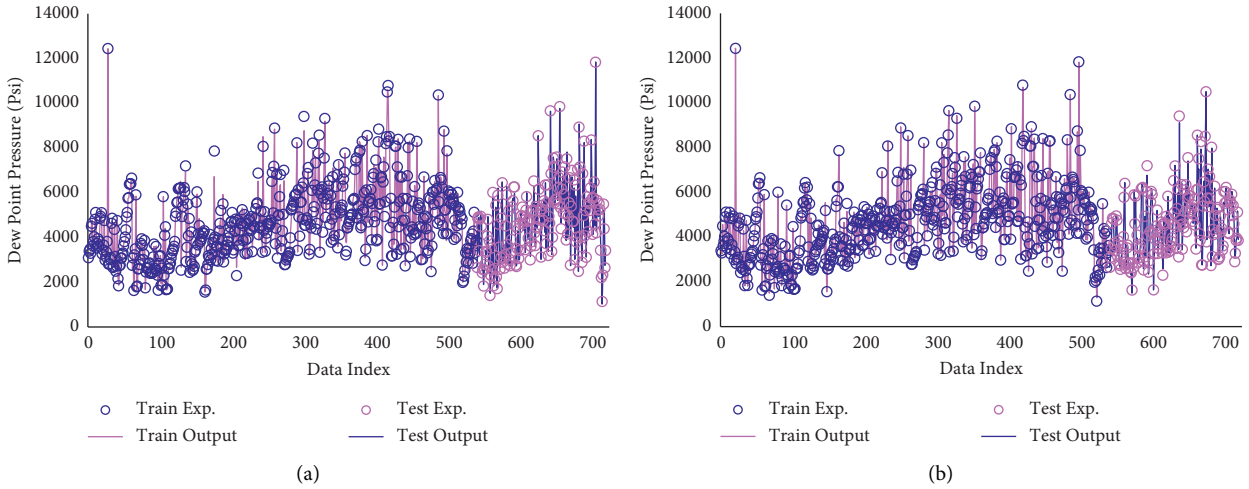

Figure 1: Simultaneous viewing of modeled and real data for (a) PSO-ANN and (b) GA-ANN models.

Furthermore, in light of finite responses, Gaussian RBFs enjoy higher biological plausibility [58].

3. GA

An initial population is created to begin the GA procedure. Then, the individuals are evaluated using fit functions before their compatibility measurement [59]. The global best satisfactory individual is identified once the error decreases below a predefined level [60]. Weaker individuals are identified and removed. This process continues until the parameters have been extracted. In order to create a new population with a smaller error, crossover and mutation are randomly implemented in the fitness evaluation phase [61, 62].

4. PSO

PSO creates an initial population of particles of random positions and velocities. Then, the particles are evaluated in fitness using a statistical fit function [63, 64]. The optimal solutions are identified once the discontinuance criteria have been met. To handle the failure to meet the discontinuance criteria, the particle positions and velocities are updated. Then, the linked parameters of the globally optimal solutions are to be updated whenever the particle has greater fitness than the globally optimal solution [65]. The optimal particle parameters are updated whenever a particle has higher fitness than the optimal one. Finally, it is required to reevaluate the next particles in the second step [66, 67].

5. Implementation and Analyses

This paper sought to estimate the DPP through GA-ANN and PSO-ANN algorithms. Theoretically, it is required to employ optimization (i.e., GA and PSO) to optimize the ANN weight and bias terms. Then, the models are evaluated statistically using the root-mean-squared error (RMSE), coefficient of determination (R^2), average relative deviation (ARD), MSE, and standard deviation (STD). These indices are defined as

$$\mathrm{MSE} = \frac{1}{N}\sum_{i=1}^{N}\left(\alpha_{\mathrm{exp}} - \alpha_{\mathrm{cal}}\right)^2, \tag{4}$$

$$\mathrm{ARD}\,(\%) = \frac{100}{N}\sum_{i=1}^{N}\frac{\alpha_{\mathrm{exp}} - \alpha_{\mathrm{cal}}}{\alpha_{\mathrm{exp}}}, \tag{5}$$

$$\mathrm{STD}_{\mathrm{error}} = \left(\frac{1}{N-1}\sum_{i=1}^{N}\left(\mathrm{error} - \overline{\mathrm{error}}\right)^2\right)^2, \tag{6}$$

$$R^2 = \frac{\left[\sum_{i=1}^{N}\left(\alpha_{\mathrm{exp}} - \alpha_{\mathrm{cal}}\right)\left(\alpha_{\mathrm{exp}} - \overline{\alpha_{\mathrm{exp}}}\right)\right]^2}{\left[\sum_{i=1}^{N}\left(\alpha_{\mathrm{exp}} - \overline{\alpha_{\mathrm{exp}}}\right)\sum_{i=1}^{N}\left(\alpha_{\mathrm{exp}} - \overline{\alpha_{\mathrm{exp}}}\right)\right]}, \tag{7}$$

$$\mathrm{RMSE} = \sqrt{\frac{1}{N}\sum_{i=1}^{N}\left(\alpha_{\mathrm{exp}} - \alpha_{\mathrm{cal}}\right)^2}, \tag{8}$$

in which N is the total number of data points, whereas α_{exp} and α_{cal} are the experimental and calculated quantities.

6. Results and Discussion

Figure 1 illustrates the experimental and estimated DPPs for the training and testing datasets. As can be seen, the models were satisfactorily efficient and effective in DPP estimation for both datasets. The proposed models seem to have high performance. However, the superior model remains yet to be identified.

Figure 2 plots the regression analysis of the experimental and estimated DPPs. As can be seen, the estimates were correlated with the experimental data. This correlation becomes linear for $R^2 = 1$. The GA-ANN model showed the highest fitness.

As shown in Figure 3, using relative deviation analysis, a good comparison between the accuracy of different models in predicting the output parameter can be obtained.

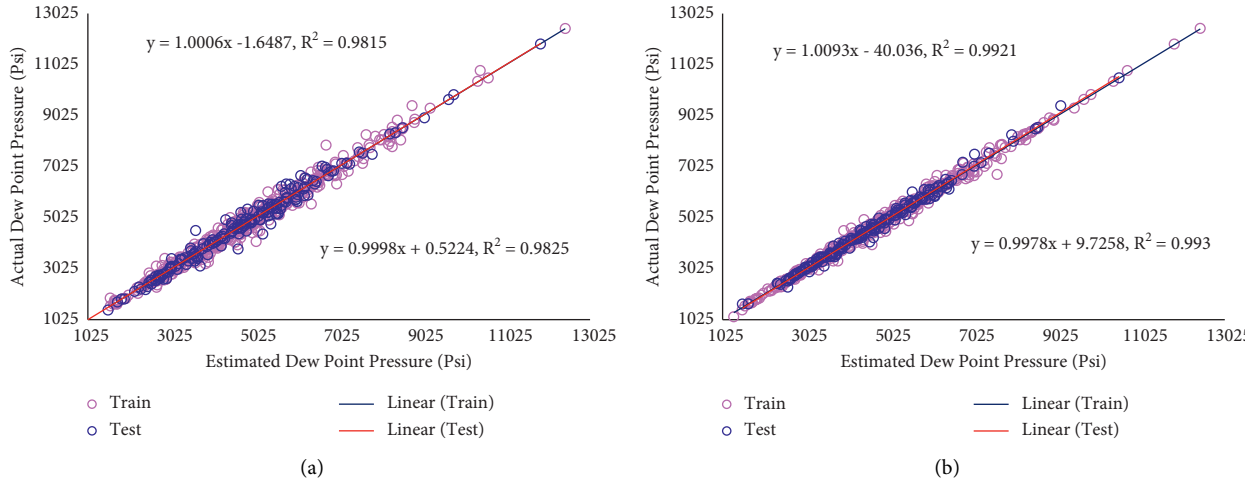

Figure 2: Linear regression on datasets modeled using (a) PSO-ANN and (b) GA-ANN.

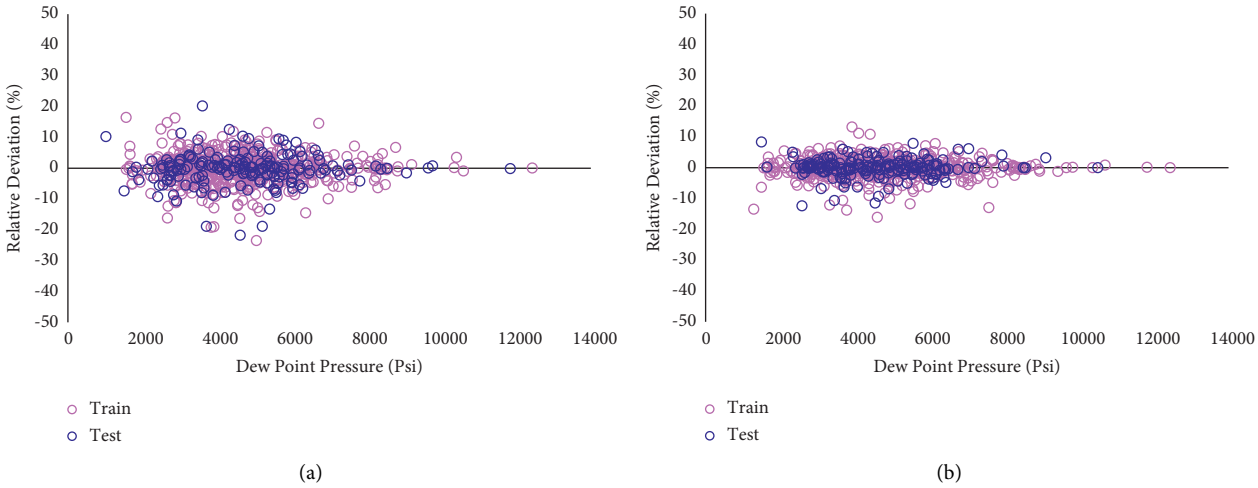

Figure 3: Relative deviation analysis to determine the accuracy of (a) PSO-ANN and (b) GA-ANN models in predicting the target parameter. The ARD, RMSE, MSE, STF, and R^2 were used to evaluate the models.

Table 1: Statistical parameters calculated for the proposed models.

Model	Dataset	R^2	MRE (%)	MSE	RMSE	STD
PSO-ANN	Train	0.982	3.457	47383.75378	217.6781	153.9872
	Test	0.981	3.484	53094.67466	230.4228	171.2903
	Total	0.982	3.464	48809.5038	230.4228	158.3618
GA-ANN	Train	0.993	2.064	20449.06595	143.0002	108.1799
	Test	0.992	1.980	17928.73343	133.8982	100.4504
	Total	0.993	2.043	19819.85672	133.8982	106.2545

Table 1 reports the MSE, RMSE, STD, ARD, and R^2 for the training, testing, and total datasets.

Figure 4 depicts the Williams plot of DP estimates to identify outlier data. The outliers have larger hat values than the warning leverage hat values and standardized residuals that are not in the range of [−3, 3].

7. Sensitivity Analysis

An ANN model relates input(s) to the output. The effect of a change in input on the output is explored using sensitivity analysis [68]. The GA-ANN model was identified as the superior algorithm. Chen et al. formulated the relevancy

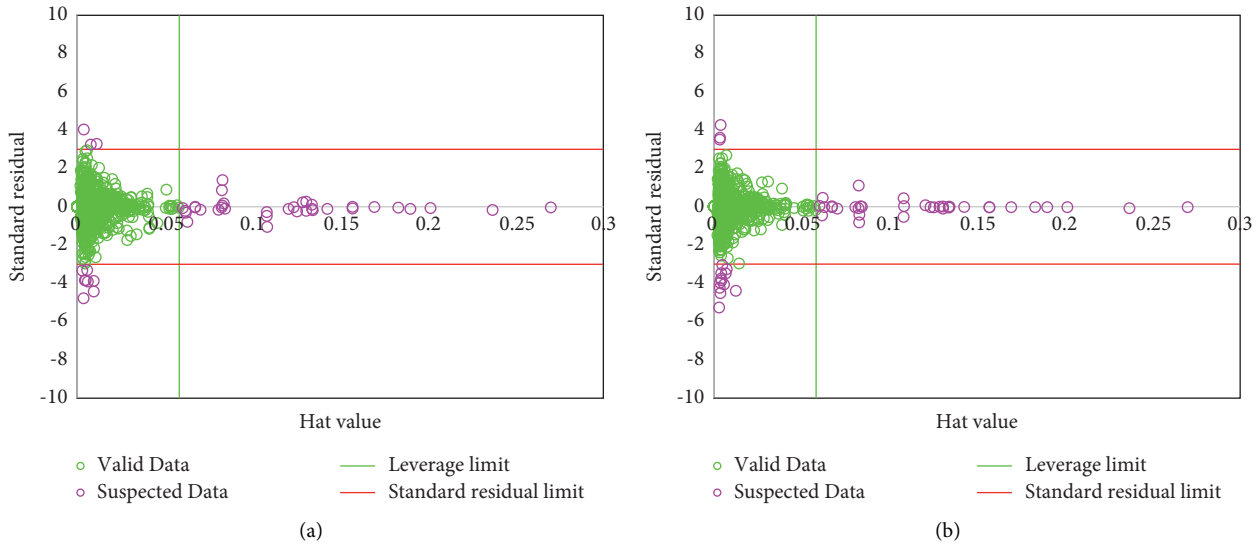

Figure 4: Williams's analysis to determine suspicious points for models (a) PSO-ANN and (b) GA-ANN.

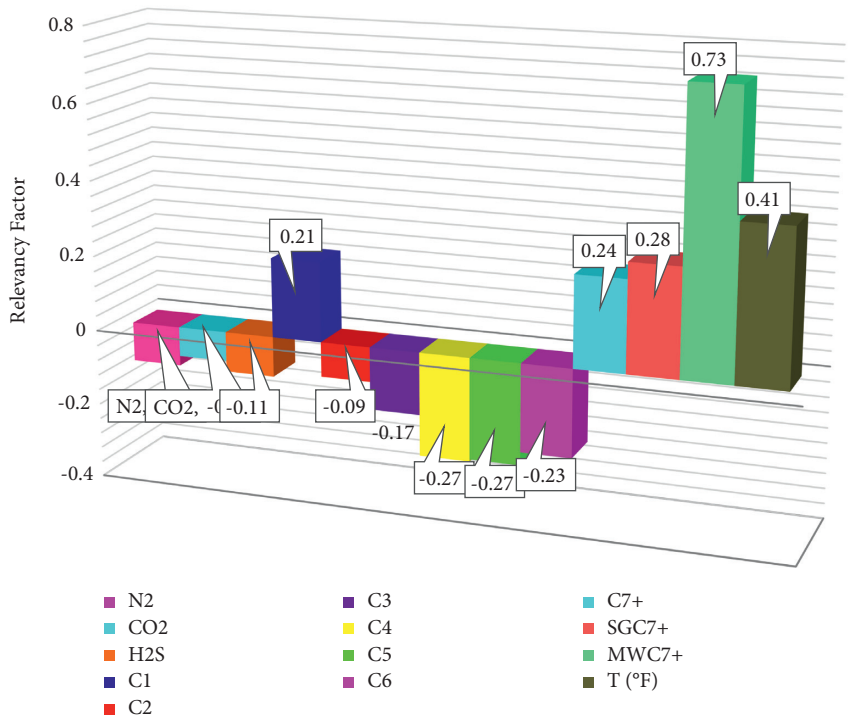

Figure 5: Sensitivity analysis on input parameters affecting the output target parameter.

factor r to identify the input with the largest effect on the output and to measure the effect of each individual input. The relevancy factor varies in the range of [−1, 1]. A larger absolute relevancy factor represents a larger effect of the corresponding input on the output [69, 70]. A positive relevancy factor implies that a rise in the input raises the output, while a negative factor would imply that an increase in the input decreases the output. According to Figure 5, the molecular weight of C_{7+}, temperature, C_1, SG C_{7+}, and C_{7+} content are directly related to DPP. Furthermore, the H_2S, CO_2, N_2, and C_2–C_6 concentrations are inversely related to the DPP. The molecular weight of C_{7+} and C_4 and C_5 content were found to pose the largest positive and negative effects on the DPP with relevancy factors of 0.73 and −0.27, respectively.

8. Conclusions

This study employed hybrid GA-ANN and PSO-ANN algorithms to estimate the DPP. A total of 721 data points were extracted from earlier works to develop the algorithms. The GA-ANN algorithm was found to outperform the PSO-ANN

framework based on mathematical leverage analysis. It efficiently estimated the experimental data with an MSE of 19819.85672, an STD of 106.2545, and R^2 of 0.993. The proposed GA-ANN model is simple and could be helpful to petroleum and chemical practitioners in the DPP estimation of a gas condensate reservoir.

Data Availability

Data references are described in the text of the article.

Conflicts of Interest

The authors declare that they have no conflicts of interest.

References

[1] M. Al-Dhamen and M. Al-Marhoun, "New correlations for dew-point pressure for gas condensate," in *SPE Saudi Arabia Section Young Professionals Technical Symposium*OnePetro, Richardson, TX, USA, 2011.

[2] M. Haji-Savameri, N. A. Menad, S. Norouzi-Apourvari, and A. Hemmati-Sarapardeh, "Modeling dew point pressure of gas condensate reservoirs: comparison of hybrid soft computing approaches, correlations, and thermodynamic models," *Journal of Petroleum Science and Engineering*, vol. 184, Article ID 106558, 2020.

[3] A. M. Elsharkawy, "Predicting the dew point pressure for gas condensate reservoirs: empirical models and equations of state," *Fluid Phase Equilibria*, vol. 193, no. 1-2, pp. 147–165, 2002.

[4] A. Najafi-Marghmaleki, A. Tatar, A. Barati-Harooni, M.-J. Choobineh, and A. H. Mohammadi, "GA-RBF model for prediction of dew point pressure in gas condensate reservoirs," *Journal of Molecular Liquids*, vol. 223, pp. 979–986, 2016.

[5] A. Delavarmoghaddam, S. A. Mirhaj, and P. L. J. Zitha, "Gas condensate productivity improvement by chemical wettability alteration," in *8th European Formation Damage Conference*OnePetro, Richardson, TX, USA, 2009.

[6] H. Rahmanifard, A. Helalizadeh, M. Ebrahimi, A. M. Shabibasl, and N. Mayahi, "Field scale and economical analysis of carbon dioxide, nitrogen, and lean gas injection scenarios in Pazanan gas condensate reservoir," *International Journal of Petroleum Engineering*, vol. 1, no. 1, pp. 62–91, 2014.

[7] M. Mohamadi-Baghmolaei, R. Azin, S. Osfouri, and S. Zendehboudi, "Evaluation of mass transfer coefficient for gas condensates in porous systems: experimental and modeling," *Fuel*, vol. 255, Article ID 115507, 2019.

[8] M. A. Sayed and G. A. Al-Muntasheri, "Mitigation of the effects of condensate banking: a critical review," *SPE Production & Operations*, vol. 31, no. 2, pp. 85–102, 2016.

[9] S. Zendehboudi, M. A. Ahmadi, L. James, and I. Chatzis, "Prediction of condensate-to-gas ratio for retrograde gas condensate reservoirs using artificial neural network with particle swarm optimization," *Energy and Fuels*, vol. 26, no. 6, pp. 3432–3447, 2012.

[10] M. A. Sayed and G. A. Al-Muntasheri, "Liquid bank removal in production wells drilled in gas-condensate reservoirs: a critical review," in *SPE International Symposium and Exhibition on Formation Damage Control*OnePetro, Richardson, TX, USA, 2014.

[11] H. Parvizi, "Field operational problems due to condensate formation," in *Retrograde Gas Reservoirs*LAP LAMBERT Academic Publishing, Sunnyvale, CA, USA, 2019.

[12] S. O. O. Baarimah, *The Effects of Well and Reservoir Parameters on Horizontal and Vertical Wells Performance in Gas Condensate Reservoir*, King Fahd University of Petroleum and Minerals (Saudi Arabia), Dhahran, Saudi Arabia, 2012.

[13] C. Herdes, T. S. Totton, and E. A. Müller, "Coarse grained force field for the molecular simulation of natural gases and condensates," *Fluid Phase Equilibria*, vol. 406, pp. 91–100, 2015.

[14] A. Kamari, A. Hemmati-Sarapardeh, S.-M. Mirabbasi, M. Nikookar, and A. H. Mohammadi, "Prediction of sour gas compressibility factor using an intelligent approach," *Fuel Processing Technology*, vol. 116, pp. 209–216, 2013.

[15] C. K. Eilerts and R. V. Smith, *Specific volumes and Phase-Boundary Properties of Separator-gas and Liquid-Hydrocarbon Mixtures*, US Department of the Interior, Bureau of Mines, Washington, DC, USA, 1942.

[16] R. H. Olds, B. H. Sage, and W. N. Lacey, "Volumetric and phase behavior of oil and gas from paloma field," *Transactions of the AIME*, vol. 160, no. 1, pp. 77–99, 1945.

[17] H. H. Reamer and B. H. Sage, "Volumetric behavior of oil and gas from a louisiana field I," *Journal of Petroleum Technology*, vol. 2, no. 9, pp. 261–268, 1950.

[18] E. I. Organick and B. H. Golding, "Prediction of saturation pressures for condensate-gas and volatile-oil mixtures," *Journal of Petroleum Technology*, vol. 4, no. 5, pp. 135–148, 1952.

[19] L. K. Nemeth and H. T. Kennedy, "A correlation of dewpoint pressure with fluid composition and temperature," *Society of Petroleum Engineers Journal*, vol. 7, no. 2, pp. 99–104, 1967.

[20] A. Crogh, *Improved Correlations for Retrograde Gases*, Texas A&M University, Bizzell, TX, USA, 1996.

[21] K. Potsch and L. Braeuer, "A novel graphical method for determining dewpoint pressures of gas condensates," in *European Petroleum Conference*OnePetro, Richardson, TX, USA, 1996.

[22] M. R. Carlson and W. Cawston, "Obtaining PVT data for very sour retrograde condensate gas and volatile oil reservoirs: a multi-disciplinary approach," in *Proceedings of the SPE Gas Technology Symposium*, Calgary, Canada, 1996.

[23] A. M. Elsharkawy, "Characterization of the plus fraction and prediction of the dewpoint pressure for gas condensate reservoirs," in *SPE Western Regional Meeting*OnePetro, Richardson, TX, USA, 2001.

[24] I. Marruffo, M. Jose, H. Jesus, and R. Gonzalo, "Correlations to determine retrograde dew pressure and C_{7+} percentage of gas condensate reservoirs on basis of production test data of eastern Venezuelan fields," in *SPE Gas Technology Symposium*OnePetro, Richardson, TX, USA, 2002.

[25] L. K. Nemeth, *A Correlation of Dew-point Pressure with Reservoir Fluid Composition and Temperature*, Texas A&M University, Bizzell, TX, USA, 1966.

[26] A. González, M. A. Barrufet, and R. Startzman, "Improved neural-network model predicts dewpoint pressure of retrograde gases," *Journal of Petroleum Science and Engineering*, vol. 37, no. 3-4, pp. 183–194, 2003.

[27] Y. Wang, R. Zou, F. Liu, L. Zhang, and Q. Liu, "A review of wind speed and wind power forecasting with deep neural networks," *Applied Energy*, vol. 304, Article ID 117766, 2021.

[28] A. Yan, Y. Hu, J. Cui et al., "Information assurance through redundant design: a novel TNU error-resilient latch for harsh

radiation environment," *IEEE Transactions on Computers*, vol. 69, no. 6, pp. 789–799, 2020.

[29] A. Yan, Z. Wu, J. Guo, and J. Song, "Novel double-node-upset-tolerant memory cell designs through radiation-hardening-by-design and layout," *IEEE Transactions on Reliability*, vol. 68, no. 1, pp. 354–363, 2018.

[30] Y. Lin, H. Song, F. Ke, W. Yan, Z. Liu, and F. Cai, "Optimal caching scheme in D2D networks with multiple robot helpers," *Computer Communications*, vol. 181, pp. 132–142, 2022.

[31] B. Wang, "Early warning method of marine products network marketing risk based on BP neural network algorithm," *Journal of Coastal Research*, vol. 103, no. SI, pp. 177–181, 2020.

[32] S. Rastogi and S. Choudhary, "Face recognition by using neural network," *Acta Informatica Malaysia*, vol. 3, no. 2, pp. 7–9, 2019.

[33] F. Mousazadeh, M. H. T. Naeem, R. Daneshfar, B. S. Soulgani, and M. Naseri, "Predicting the condensate viscosity near the wellbore by ELM and ANFIS-PSO strategies," *Journal of Petroleum Science and Engineering*, vol. 204, Article ID 108708, 2021.

[34] A. Lekomtsev, A. Keykhosravi, M. B. Moghaddam, R. Daneshfar, and O. Rezvanjou, "On the prediction of filtration volume of drilling fluids containing different types of nanoparticles by ELM and PSO-LSSVM based models," *Petroleum*, In press, 2021.

[35] S. Alizadeh, I. Alruyemi, R. Daneshfar, M. Mohammadi-Khanaposhtani, and M. Naseri, "An insight into the estimation of drilling fluid density at HPHT condition using PSO-, ICA-, and GA-LSSVM strategies," *Scientific Reports*, vol. 11, no. 1, pp. 1–14, 2021.

[36] K. Shang, Z. Chen, Z. Liu et al., "Haze prediction model using deep recurrent neural network," *Atmosphere*, vol. 12, no. 12, Article ID 1625, 2021.

[37] Z. Zhang, J. Tian, W. Huang, L. Yin, W. Zheng, and S. Liu, "A haze prediction method based on one-dimensional convolutional neural network," *Atmosphere*, vol. 12, no. 10, Article ID 1327, 2021.

[38] R. Prasad and K. D. Yadav, "Use of response surface methodology and artificial neural network approach for methylene blue removal by adsorption onto water hyacinth," *Water Conserv Manag WCM*, vol. 4, pp. 73–79, 2020.

[39] M. Lak Kamari, H. Isvand, and M. Alhuyi Nazari, "Applications of multi-criteria decision-making (MCDM) methods in renewable energy development: a review," *Renewable Energy Research and Application*, vol. 1, no. 1, pp. 47–54, 2020.

[40] H. Pourderogar, H. Harasii, R. Alayi, S. H. Delbari, M. Sadeghzadeh, and A. Javaherbakhsh, "Modeling and technical analysis of solar tracking system to find optimal angle for maximum power generation using MOPSO algorithm," *Renewable Energy Research and Application*, vol. 1, no. 2, pp. 211–222, 2020.

[41] M. B. Vanani, R. Daneshfar, and E. Khodapanah, "A novel MLP approach for estimating asphaltene content of crude oil," *Petroleum Science and Technology*, vol. 37, no. 22, pp. 2238–2245, 2019.

[42] R. Daneshfar, F. Keivanimehr, M. Mohammadi-Khanaposhtani, and A. Baghban, "A neural computing strategy to estimate dew-point pressure of gas condensate reservoirs," *Petroleum Science and Technology*, vol. 38, no. 10, pp. 706–712, 2020.

[43] F. Jalali, Y. Abdy, and M. K. Akbari, "Using artificial neural Network's capability for estimation of gas condensate Reservoir's dew point pressure," in *EUROPEC/EAGE Conference and Exhibition*OnePetro, Richardson, TX, USA, 2007.

[44] O. N. Godwin, "A new analytical method for predicting dew point pressures for gas condensate reservoirs," in *Nigeria Annual International Conference and Exhibition*OnePetro, Richardson, TX, USA, 2012.

[45] A. Alzahabi, A. El-Banbi, A. Alexandre Trindade, and M. Soliman, "A regression model for estimation of dew point pressure from down-hole fluid analyzer data," *Journal of Petroleum Exploration and Production Technology*, vol. 7, no. 4, pp. 1173–1183, 2017.

[46] M. Mirzaie, H. Esfandyari, and A. Tatar, "Dew point pressure of gas condensates, modeling and a comprehensive review on literature data," *Journal of Petroleum Science and Engineering*, vol. 211, Article ID 110072, 2021.

[47] A. H. Elsheikh, S. W. Sharshir, M. Abd Elaziz, A. E. Kabeel, W. Guilan, and Z. Haiou, "Modeling of solar energy systems using artificial neural network: a comprehensive review," *Solar Energy*, vol. 180, pp. 622–639, 2019.

[48] M. Zare, H. R. Pourghasemi, M. Vafakhah, and B. Pradhan, "Landslide susceptibility mapping at Vaz Watershed (Iran) using an artificial neural network model: a comparison between multilayer perceptron (MLP) and radial basic function (RBF) algorithms," *Arabian Journal of Geosciences*, vol. 6, no. 8, pp. 2873–2888, 2013.

[49] R. Sharaf, A. Noureldin, A. Osman, and N. El-Sheimy, "Online INS/GPS integration with a radial basis function neural network," *IEEE Aerospace and Electronic Systems Magazine*, vol. 20, no. 3, pp. 8–14, 2005.

[50] S. Mohamadi, M. Ehteram, and A. El-Shafie, "Accuracy enhancement for monthly evaporation predicting model utilizing evolutionary machine learning methods," *International journal of Environmental Science and Technology*, pp. 1–24, 2020.

[51] A. Najah, A. El-Shafie, O. A. Karim, and A. H. El-Shafie, "Application of artificial neural networks for water quality prediction," *Neural Computing and Applications*, vol. 22, no. 1, pp. 187–201, 2013.

[52] A. Massa, G. Oliveri, M. Salucci, N. Anselmi, and P. Rocca, "Learning-by-examples techniques as applied to electromagnetics," *Journal of Electromagnetic Waves and Applications*, vol. 32, no. 4, pp. 516–541, 2018.

[53] M. Sharifzadeh, A. Sikinioti-Lock, and N. Shah, "Machine-learning methods for integrated renewable power generation: a comparative study of artificial neural networks, support vector regression, and Gaussian Process Regression," *Renewable and Sustainable Energy Reviews*, vol. 108, pp. 513–538, 2019.

[54] E. Bou Assi, *Towards Accurate Forecasting of Epileptic Seizures: Artificial Intelligence and Effective Connectivity Findings*, École Polytechnique de Montréal, Montreal, Canada, 2018.

[55] E. S. Siah, *Hybrid Modeling of Electromagnetic Interference on Circuit and Structure Topologies*, University of Michigan, Ann Arbor, MI, USA, 2005.

[56] J. Soltani Rad, *A Comprehensive Study on Tool Condition Monitoring Using Time-Frequency Transformation and Artificial Intelligence*, Concordia University, Montreal, Canada, 2015.

[57] A. Mudgal and R. Singh, "A hybrid method of medical image de-nosing using subtraction transform and radial biases neural network," *International Journal of Computer Science and Engineering*, vol. 3, no. 9, pp. 54–59, 2015.

[58] R. Yokota, L. A. Barba, and M. G. Knepley, "PetRBF—a parallel O(N) algorithm for radial basis function interpolation with Gaussians," *Computer Methods in Applied Mechanics and Engineering*, vol. 199, no. 25–28, pp. 1793–1804, 2010.

[59] J. Genlin, "Survey on genetic algorithm," *Computer Applications and Software*, vol. 2, no. 1, pp. 69–73, 2004.

[60] C. R. Houck, J. Joines, and M. G. Kay, "A genetic algorithm for function optimization: a Matlab implementation," *Ncsu-ie tr*, vol. 95, no. 9, pp. 1–10, 1995.

[61] S. Mirjalili, "Genetic algorithm," in *Evolutionary Algorithms and Neural Networks*, pp. 43–55, Springer, Berlin, Germany, 2019.

[62] M. Yong-Jie and Y. Wen-Xia, "Research progress of genetic algorithm," *Application Research of Computers*, vol. 29, no. 4, pp. 1201–1206, 2012.

[63] R. Poli, J. Kennedy, and T. Blackwell, "Particle swarm optimization," *Swarm Intelligence*, vol. 1, no. 1, pp. 33–57, 2007.

[64] Y. Shi and R. C. Eberhart, "Empirical study of particle swarm optimization," in *Proceedings of the 1999 Congress on Evolutionary Computation-CEC99 (Cat. No. 99TH8406)*, Washington, DC, USA, 1999.

[65] Y. Shi, "Particle swarm optimization: developments, applications and resources," in *Proceedings of the 2001 Congress on Evolutionary Computation*, Seoul, Republic of Korea, May 2001.

[66] D. Bratton and J. Kennedy, "Defining a standard for particle swarm optimization," in *Proceedings of the 2007 IEEE Swarm Intelligence Symposium*, Honolulu, HI, USA, April 2007.

[67] F. vandenBergh and A. P. Engelbrecht, "A cooperative approach to particle swarm optimization," *IEEE Transactions on Evolutionary Computation*, vol. 8, no. 3, pp. 225–239, 2004.

[68] R. Setiawan, R. Daneshfar, O. Rezvanjou, S. Ashoori, and M. Naseri, "Surface tension of binary mixtures containing environmentally friendly ionic liquids: insights from artificial intelligence," *Environment, Development and Sustainability*, vol. 23, no. 12, pp. 17606–17627, 2021.

[69] D. Ahangari, R. Daneshfar, M. Zakeri, S. Ashoori, and B. S. Soulgani, "On the prediction of geochemical parameters (TOC, S1 and S2) by considering well log parameters using ANFIS and LSSVM strategies," *Petroleum*, In press, 2021.

[70] R. Syah, M. H. T. Nazeem, R. Daneshfar, H. Dehdar, and B. S. Soulgani, "On the prediction of methane adsorption in shale Using grey wolf optimizer support vector machine approach," *Petroleum*, In press, 2021.